REGULARIZED DOPPLER RADAR IMAGING FOR TARGET IDENTIFICATION IN ATMOSPHERIC CLUTTER

Philippe Ciuciu

CEA/SHFJ, 4 place du Général Leclerc
91 406 Orsay, France
ciuciu@shfj.cea.fr

Jérôme Idier

IRCCyN, 1 rue de la Noë, BP 92101
44321 Nantes cedex 3, France
Jerome.Idier@irccyn.ec-nantes.fr

ABSTRACT

We develop a method for the formation of Doppler radar images with enhanced features. This problem, when studied as an adaptive spectral estimation problem, is particularly *ill-posed* because of the small number of data. Our approach is based on a regularized estimation of *depth-frequency* images which combines a high-resolution Fourier model of the observations with prior information about the nature of the features of interest. We first derive an appropriate model and a regularized criterion for meteorological clutter restoration before addressing the extension to the identification of spot-like targets superimposed to this clutter. We also adapt quasi-Newton algorithms based on Half-Quadratic regularization [1, 2] for the computation of the solution. The practical interest of our approach is validated on simulated and real data.

1. INTRODUCTION

The problem of adaptive spectral estimation has received considerable attention in the signal processing community [3, 4, 5] since it came up in various fields of engineering, especially in radar Doppler imaging. In this context, it consists in searching for a series of spatially depth-wise juxtaposed spectra given the discrete time data, extracted for any depth of interest. The present paper focuses on short-time estimation since only eight time points of complex-valued pulsed Doppler signals are available to estimate *each* spectrum. Two complementary problems are then studied.

Section 2 focuses on estimating a series of spectra of atmospheric clutter (rain, sea, mixed clutter) with a large variability in terms of spectral content and number of modes. Given a small number of data points, periodogram-based estimates are unreliable. Long AR models have been investigated using quadratic regularization to account for *spectral smoothness* and *depth continuity* [6, 3, 5]. Unfortunately, quadratic penalization oversmoothes discontinuities between different clutters. To overcome these limitations, we propose a depth-frequency analysis in a nonparametric framework. In [7], we have developed a regularized approach that integrates spectral smoothness for the estimation of a single spectrum. Here, we propose a 2D extension to account for depth continuity as well. The depth-frequency image solution is defined as the global minimizer of a convex criterion, regularized in both directions (depth and frequency) using a nonquadratic penalty term.

Section 3 addresses the problem of restoration of targets superimposed on atmospheric clutter. The proposed approach generalizes the mixed spectrum estimation method proposed in [7]. It amounts to estimating two depth-frequency distributions: one for the targets and one for the clutters. Since target spectra are mostly spiky, a separable penalty term is used to enhance this feature. Finally, the pairs of mixed spectra that result from global optimization of a unique criterion are summed up to provide a map that displays both the targets and the clutter. Efficient numerical solution is achieved through 2D extensions of block-coordinate descent based on HQ regularization [1, 2]. These methods are matched to the complex nature of the estimated quantities. In Section 5, results on synthetic and real Doppler signals are presented.

2. ATMOSPHERIC CLUTTER IMAGING

2.1. Problem statement

In radar Doppler imaging, the data consist of a set of complex-valued signals $\mathcal{Y} = [\boldsymbol{y}_1, \ldots, \boldsymbol{y}_M]$, spatially depth-wise juxtaposed in M bins, each reflecting a certain depth range. Following [4, 7], each short-time vector of data $\boldsymbol{y}_m$ is assumed to be a truncated subset of a complex time series $(y_{nm})_{n\in\mathbb{Z}}$. Moreover, it is supposed to be independent from its neighbors $\boldsymbol{y}_{m\pm1}$. Fig. 1 gives a Gaussian simulated example over $M = 96$ range bins for which $N = 8$ data are observed per bin.

Depth-frequency estimation is addressed as the depth-wise extension of spectral analysis. For short-time data sets, this issue can be tackled as a Fourier synthesis problem [4, 7]. Similarly, our goal is to search for the energy distribution of $(y_{nm})_{n\in\mathbb{Z}}$ in the frequency domain. The harmonic frequency model is usually considered for this task. Assuming that the distribution of spectral amplitudes $X_m(\nu)$ is continuous with respect to frequencies ν, the inverse discrete-time Fourier transform links the unknown function $X_m \in L^2_{\mathbb{C}}[0, 1]$ to the finite energy series $(y_{nm})_{n\in\mathbb{Z}}$ according to

$$y_{nm} = \int_0^1 X_m(\nu)\; e^{2j\pi\nu n}\; d\nu. \tag{1}$$

Spectral estimation is thus a discrete-time continuous-frequency problem, consisting in recovering $X_m(\nu)$ given y_{nm} for $n \in \mathbb{N}_N = \{0, \ldots, N-1\}$. Following [4, 7], we resort to a discrete frequency approximation using a large number of sinusoids, say $P \gg N$, at equally sampled frequencies $p/P, p \in \mathbb{N}_P$. The approximation of (1) then reads

$$y_{nm} = \sum_{p=0}^{P-1} X_{pm}\; w_0^{pn},\; n \in \mathbb{N}_N, \tag{2}$$

where $w_0 = \exp(2j\pi/P)$ and $X_{pm} \in \mathbb{C}$ are the unknown spectral amplitudes. In vector-matrix form, (2) rereads:

$$\boldsymbol{y}_m = W_{NP}\boldsymbol{X}_m, \tag{3}$$

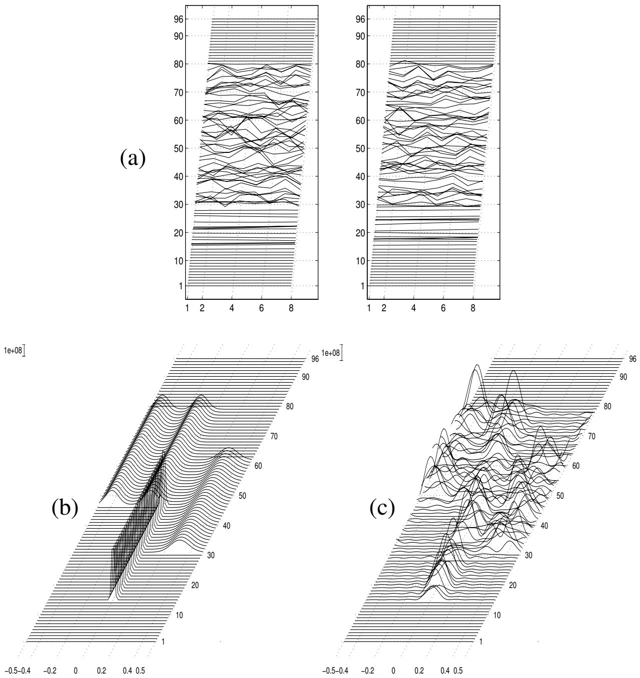

Fig. 1. Simulated data over 96 range bins with 8 Doppler pulsed signals per bin. (a) real and imaginary parts of the data. (b) the series of true spectra. The narrow zero-mean spectra characterizes ground clutter (bin 15 to 47). Rain clutter presents broader single-mode spectra (bin 31 to 63). Sea echos exhibit two maxima (bin 47 to 79). (c) the associated periodograms.

where $W_{NP} = [w_0^{np}]_{n\in\mathbb{N}_N}^{p\in\mathbb{N}_P}$ and $\boldsymbol{X}_m = [X_{0,m}, \dots, X_{P-1,m}]^{\mathrm{t}}$.

For the whole dataset, concatenation of equation (3) in M depth range bins yields $\mathcal{Y} = \mathcal{W}\mathcal{X}$ with $\mathcal{W} = \mathrm{diag}[W_{NP}]$ and $\mathcal{X} = [\boldsymbol{X}_1, \dots, \boldsymbol{X}_M]$, which states the 2D relationship between the observations and the unknown Fourier coefficients (or complex spectra). Since $N \ll P$, this system is underdetermined, and there exists an infinite number of solutions in the least squares sense. The problem is now to incorporate structural information to overcome the underdeterminacy in an appropriate way.

2.2. Estimate

Following [4, 7], we use a penalized approach. That means the estimate $\widehat{\mathcal{X}}$ is the complex-valued Doppler image given by $\widehat{\mathcal{X}} = \arg\min \mathcal{J}(\mathcal{X})$, where

$$\mathcal{J}(\mathcal{X}) = \|\mathcal{Y} - \mathcal{W}\mathcal{X}\|^2 + \lambda\mathcal{R}(\mathcal{X}).$$

From the Bayesian viewpoint, $\widehat{\mathcal{X}}$ corresponds to the MAP (Maximum *A Posteriori*) estimate [4], and its componentwise squared modulus $|\widehat{\mathcal{X}}|^2$ defines the estimate of the series of power spectra. The hyperparameter $\lambda > 0$ controls the trade-off between the closeness to the data and the confidence in a structural prior model embodied in $\mathcal{R}$. Here, spectral smoothness and depth continuity define our prior information on the atmospheric clutter $\mathcal{X}$. Spectral regularity involves each vector $\boldsymbol{X}_m$ separately, whereas depth continuity involves neighbor range bins, but both are related to the power spectra, *i.e.,* to positive distributions. As a consequence, $\mathcal{R}$ is chosen *circular*, that is

$$\mathcal{R}(\mathcal{X}) = \mathcal{R}(\boldsymbol{X}_1, \cdots, \boldsymbol{X}_P) = \mathcal{R}(\boldsymbol{\rho}_1, \cdots, \boldsymbol{\rho}_P)$$

with $\boldsymbol{\rho}_m = |\boldsymbol{X}_m| = [\rho_{1m}, \dots, \rho_{Pm}]^{\mathrm{t}}$. For computational simplicity, we focus on convex and continuously differentiable (C^1) energies $\mathcal{R}$ and $\mathcal{J}$.

2.3. Markovian depth-frequency regularization

In [7], we have proposed the following circular and convex penalty term to enforce spectral smoothness:

$$R_{\mathrm{S}}(\boldsymbol{X}_m) = \sum_{p=0}^{P-1} \left(\mu_{\mathrm{S}}\phi_1(\rho_{p+1,m} - \rho_{pm}) + \phi_2(\rho_{pm})\right), \qquad (4)$$

where $\mu_{\mathrm{S}} \geq 0$ tunes the amount of smoothness, $\phi_2 : \mathbb{R}_+ \mapsto \mathbb{R}$, and $\rho_{P,m} = \rho_{0,m}$ because of the 1-periodicity of the discrete Fourier transform. As stated in [7, Corollary 1], function R_{S} is circular, *i.e.,* $R_{\mathrm{S}}(\boldsymbol{X}_m) = R_{\mathrm{S}}(\boldsymbol{\rho}_m)$ and convex, provided that:

- ϕ_1 is even and convex, (5a)
- ϕ_2 is convex and nondecreasing, (5b)
- $\mu_{\mathrm{S}} \leq \mu_{\sup} = \phi_2'(0^+)/2\phi_1'(\infty)$. (5c)

Inequality (5c) gives an upper bound on the smoothness level that can be chosen while maintaining convexity of R_{S}. Since $\mu_{\sup} > 0$ requires $\phi_2'(0^+) > 0$, $\phi_2(|\cdot|)$ and R_{S} are not C^1 at zero. For $\phi_2(u) = u$, a C^1 approximation is [7]

$$R_{\mathrm{S},\,\varepsilon}(\boldsymbol{X}_m) = \sum_{p=0}^{P-1} \left(\mu_{\mathrm{S}}\phi_1(q_{p+1,m} - q_{p,m}) + q_{p,m}\right), \qquad (6)$$

where $q_{pm} = \phi_\varepsilon(\rho_{pm})$, $\phi_\varepsilon(x) = \sqrt{\varepsilon^2 + |x|^2}$, and $\varepsilon > 0$. Function $R_{\mathrm{S},\,\varepsilon}$ is also circular and its convexity is proven in [7, Corollary 2] under conditions (5a)–(5c).

Spectral regularity and depth continuity are simultaneously taken into account in a natural extension of (6) given by

$$\mathcal{R}(\mathcal{X}) = \sum_{m=1}^{M} R_{\mathrm{S},\,\varepsilon}(\boldsymbol{X}_m) + \mu_{\mathrm{T}} \sum_{m=1}^{M-1}\sum_{p=0}^{P-1} \phi_3(q_{p,m+1} - q_{pm}), \quad (7)$$

where ϕ_3 is also convex, and $\mu_{\mathrm{T}} \geq 0$ tunes the amount of depth continuity. Proceeding as in the previous 1D case, a straightforward extension of (5c) that guarantees convexity of $\mathcal{R}$ is:

$$\mu_{\mathrm{S}} \leq \frac{a}{2\phi_2'(\infty)} \text{ and } \mu_{\mathrm{T}} \leq \frac{(1-a)}{2\phi_3'(\infty)}, \quad \text{for } a \in [0,\, 1]. \quad (8)$$

In practice, ϕ_1 and ϕ_3 are chosen quadratic around zero to avoid ringing artifacts, and linear at infinity, to restore spectral and/or depth discontinuities [8, 9]. Among this set of functions, we retain the hyperbolic potentials: $\phi_{1,3}(\rho) = \sqrt{\tau_{1,3}^2 + \rho^2}$. Given these choices, $\mathcal{R}$ is convex if μ_{S} and $\mu_{\mathrm{T}} \leq 1/4$, for a fair compromise between spectral regularity and depth continuity ($a = 1/2$). Finally, the whole set of hyperparameters is $\boldsymbol{\theta} = (\lambda,\, \mu_{\mathrm{S}},\, \tau_1,\, \mu_{\mathrm{T}},\, \tau_3,\, \varepsilon)$.

3. TARGET IDENTIFICATION IN ATMOSPHERIC CLUTTER

3.1. Depth-frequency mixed model

A *mixed* spectrum consists of both frequency peaks and smooth spectral components. Mixed spectrum estimation has been addressed in [7]. Here, we propose a depth-wise extension for the restoration of a series of such spectra. Following [7], each vector $\boldsymbol{X}_m$ is split into two sets of unknown variables: the frequency peaks $\boldsymbol{X}_m^{\text{L}}$ and the smoother components $\boldsymbol{X}_m^{\text{S}}$. Then, the observation model reads $\boldsymbol{y}_m = W_{NP}(\boldsymbol{X}_m^{\text{L}} + \boldsymbol{X}_m^{\text{S}})$ in range bin m. Given the whole set of range bins, adequation of the model to the data is measured by

$$\mathcal{Q}(\mathcal{X}) = \|\mathcal{Y} - \mathcal{W}(\mathcal{X}^{\text{L}} + \mathcal{X}^{\text{S}})\|^2 = \|\mathcal{Y} - \mathcal{W}\mathcal{X}\,[1, 1]^{\text{t}}\,\|^2,$$

where $\mathcal{X}^{\text{L}} = [\boldsymbol{X}_1^{\text{L}}, \dots, \boldsymbol{X}_M^{\text{L}}]$, $\mathcal{X}^{\text{S}} = [\boldsymbol{X}_1^{\text{S}}, \dots, \boldsymbol{X}_M^{\text{S}}]$ and $\mathcal{X} = [\mathcal{X}^{\text{L}} \,|\, \mathcal{X}^{\text{S}}]$ is a $P \times 2M$ complex matrix. In this form, the problem is still ill-posed. The construction of the regularization term is now detailed.

3.2. Estimate

Minimizing a penalized criterion defined from (7) does not allow to retrieve spectral peaks embedded in a broadband background [7]. According to [7], mixed spectra restoration is achieved by means of a *compound* penalized criterion

$$\mathcal{J}_{\text{M}}(\mathcal{X}) = \mathcal{Q}_{\text{M}}(\mathcal{X}) + \lambda_{\text{L}}\mathcal{R}_{\text{L}}(\mathcal{X}^{\text{L}}) + \lambda_{\text{S}}\mathcal{R}_{\text{S}}(\mathcal{X}^{\text{S}}), \quad (\lambda_{\text{L}}, \lambda_{\text{S}}) > 0 \quad (9)$$

where $\mathcal{R}_{\text{L}}$ is designed to enhance spectral peaks and $\mathcal{R}_{\text{S}}$ takes the form of (7). Akin to [4, 7], we introduce a *separable* circular convex energy $\mathcal{R}_{\text{L}}$ to reconstruct a line spectrum $\boldsymbol{X}_m^{\text{L}}$ in all range bins m. In the context of Doppler radar imaging, such a penalization becomes

$$\mathcal{R}_{\text{L}}(\mathcal{X}^{\text{L}}) = \sum_{m=1}^{M} \sum_{p=0}^{P-1} \phi_0(\rho_{pm}^{\text{L}}),$$

where $\rho_{pm}^{\text{L}} = \left|X_{pm}^{\text{L}}\right|$, and ϕ_0 is hyperbolic as well as $\phi_{1,3}$. Since ϕ_0 is convex and increasing on R_+, $\mathcal{R}_{\text{L}}$ is convex [7, Proposition 1]. Given that $\mathcal{R}_{\text{S}}$ is also convex and C^1, the global criterion $\mathcal{J}_{\text{M}}$ inherits the same properties. Its global minimizer is defined by

$$\widehat{\mathcal{X}} = [\widehat{\mathcal{X}}_{\text{L}} \,|\, \widehat{\mathcal{X}}_{\text{S}}] = \arg\min_{\mathcal{X}} \mathcal{J}_{\text{M}}(\mathcal{X}).$$

In the Bayesian framework adopted in [4], $(\widehat{\mathcal{X}}_{\text{L}}, \widehat{\mathcal{X}}_{\text{S}})$ corresponds to the joint MAP estimate. Finally, the Doppler image solution is the componentwise squared modulus of the superposition $\widehat{\mathcal{X}}_{\text{L}} + \widehat{\mathcal{X}}_{\text{S}}$. Note that eight parameters $\boldsymbol{\theta}_{\text{M}} = (\lambda_{\text{L,S}}, \tau_{0,1,3}, \mu_{\text{S,T}}, \varepsilon)$ have to be tuned for the estimation of a series mixed spectra.

4. COMPUTATIONAL ISSUE

We now discuss the minimization stage of $\mathcal{J}$ and $\mathcal{J}_{\text{M}}$. In [1], we have introduced powerful minimization block-coordinate descent methods for line and smooth spectra restoration. They rely upon two forms of *half-quadratic (HQ) regularization*: Geman & Reynolds' construction and Geman & Yang's one, respectively. the second one allows to derive convex and C^1 HQ criteria for Markovian penalty terms such as (6). For this reason, the second algorithm has been generalized for mixed spectra restoration in [2]. Convergence proofs have been stated for convex and C^1 criteria such as $\mathcal{J}$ and $\mathcal{J}_{\text{M}}$. As shown in [10], the 2D depth-frequency extensions for estimation of clutter and target-clutter radar images are straightfoward for the following reasons. First, there is no correlation between adjacent range bins in the observation model. Second, the penalization terms involving the frequency and depth directions in (7) do not interact. Note that these techniques are quite similar to the quasi-Newton algorithm developed in [11] where no convergence proof is given.

5. EXPERIMENTAL RESULTS

5.1. Simulated example

The solution spectra have been computed on $P = 64$ frequency points. In practice, taking $P > 64$ does not markedly improve the resolution, while it increases the computational burden.

Fig. 2 shows a comparison between our solution and the spectra series yielded by the long AR regularized technique [5]. In our approach, the hyperparameter values have been empirically selected after several trials, as those that minimize the L_1 distance between true and estimated spectra. Consequently, the hyperparameters $\boldsymbol{\theta} = (0.5, 0.4, 400, 6, 10^3)$ have been retained. Note that spectral smoothness is less enforced than depth continuity since $\mu_{\text{S}} \ll \mu_{\text{T}}$: this allows to account for the presence of the narrow band ground clutter. Moreover, convexity of the corresponding penalization $\mathcal{R}$ is not ensured since conditions (8) are not fullfiled. In practice, the restoration of mixed clutters as those in Fig. 2 requires nonconvex energies since $(\mu_{\text{S}} = .4, \mu_{\text{T}} = 6) > 1/4$.

In the AR technique, there are only two hyperparamters, $\beta_{\text{S}} = \lambda\mu_{\text{S}}$ and $\beta_{\text{D}} = \lambda\mu_{\text{D}}$ that have been set using the same empirical rule[1], leading to $(\beta_{\text{S}}, \beta_{\text{D}}) = (0.12, 250)$. A qualitative comparison with Fig. 1 leads to four conclusions.

- The effect of regularization is obvious. Spectra estimated with the AR method or our technique are closer to the true ones compared to the periodograms.
- The ground clutter is estimated with a high resolution by both regularized methods.
- The sudden transitions at the beginning and the end of the ground clutter are over-smoothed by the AR method whereas they are preserved by our approach. In addition, the rain clutter and sea echos are enhanced by our approach.
- The computation of our depth-frequency image requires three times more parameters than using the AR method.

Finally, remark that heterogeneous clutters are better separated with a nonquadratic energy.

A quantitative comparison has been achieved by evaluating L_1 distances between true and estimated spectra. The results show an improvement of about 25 % from periodograms to the AR method, and 20 % from the AR solution to the proposed one.

5.2. Real data of Doppler radar imaging

The proposed technique for estimation of a series of mixed spectra is tested on real data[2]. The recording ($M = 48$, $N = 8$)

[1] an unsupervised extension is proposed in [5] where $(\beta_{\text{S}}, \beta_{\text{D}})$ are automatically selected using a maximum likelihood strategy.

[2] The authors wish to thank Daniel Muller (Thales Air-Defense, Bagneux, France) for providing the Doppler radar data presented in the paper.

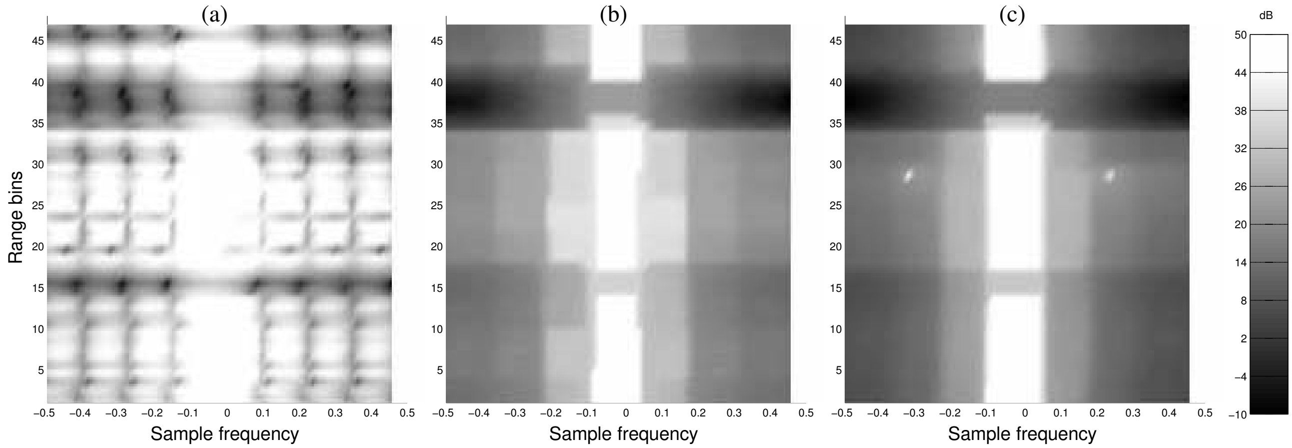

Fig. 3. (a) series of periodograms, (b) result from clutter estimation technique, (c): sequence restored by mixed estimation.

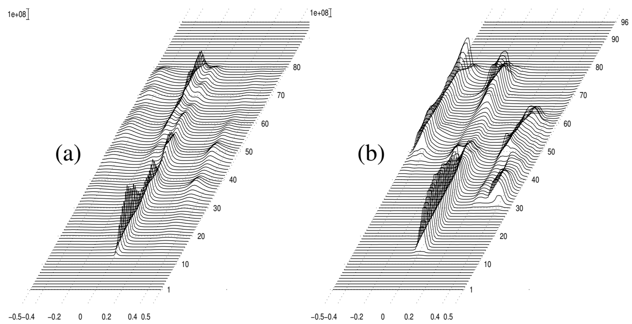

Fig. 2. Mixed clutter estimates: (a) regularized long AR solution of [5]. (b) our clutter imaging technique.

was composed of a meteorological clutter and an isolated target. Fig. 3(a) shows that the periodogram was not able to detect the target. The result of the clutter characterization technique is depicted in Fig. 3(b). The depth-frequency shape of the clutter is accurately restored but the target is lost as well. The clutter estimate has been computed using $P = 64$ and an empirically chosen vector $\boldsymbol{\theta}$. The joint MAP solution (*i.e.,* $|\widehat{\mathcal{X}}_{\mathrm{L}} + \widehat{\mathcal{X}}_{\mathrm{S}}|^2$) is presented in Fig. 3(c). The isolated target clearly appears in range bin $m = 29$, through spots at $f_1 = -.29$ and $f_2 = .25$. This depth-frequency image has been computed with the same set $(\tau_{,1,3}, \mu_{\mathrm{S,T}}, \varepsilon)$. Two additional hyperparameters $(\lambda_{\mathrm{L}}, \lambda_{\mathrm{S}})$ appear in (9). It is *a priori* useful that choose values of λ_{L} and λ_{S} to have the same order of magnitude, otherwise the over-penalized term would yield a vanishing Doppler image.

6. CONCLUSION

This communication addresses depth-frequency spectral estimation in the context of Doppler radar imaging within the regularization framework. Two different problems were tackled. The first was the reconstruction of atmospheric clutters that present rather smooth shapes. The second one was an extension to the identification of spiky objects embedded in such clutters. We proposed solutions to both by the definition of an appropriate regularized criteria and demonstrated the validity of the approach on real data.

7. REFERENCES

[1] P. Ciuciu, J. Idier, and J.-F. Giovannelli, "Markovian high resolution spectral analysis," in *Proc. IEEE ICASSP*, Phoenix, AZ, Mar. 1999, pp. 1601–1604.

[2] P. Ciuciu and J. Idier, "A Half-Quadratic block-coordinate descent method for spectral estimation," *Signal Processing*, vol. 82, no. 7, pp. 941–959, July 2002.

[3] G. Kitagawa and W. Gersch, "A smoothness priors time-varying AR coefficient modeling of nonstationary covariance time series," *IEEE Trans. Automat. Contr.*, vol. AC-30, no. 1, pp. 48–56, Jan. 1985.

[4] M. D. Sacchi, T. J. Ulrych, and C. J. Walker, "Interpolation and extrapolation using a high-resolution discrete Fourier transform," *IEEE Trans. Signal Processing*, vol. 46, no. 1, pp. 31–38, Jan. 1998.

[5] J.-F. Giovannelli, J. Idier, G. Desodt, and D. Muller, "Regularized adaptive long autoregressive spectral analysis," *IEEE Trans. Geosci. Remote Sensing*, vol. 39, no. 10, pp. 2194–2202, Oct. 2001.

[6] G. Kitagawa and W. Gersch, "A smoothness priors long AR model method for spectral estimation," *IEEE Trans. Automat. Contr.*, vol. AC-30, no. 1, pp. 57–65, Jan. 1985.

[7] P. Ciuciu, J. Idier, and J.-F. Giovannelli, "Regularized estimation of mixed spectra using a circular Gibbs-Markov model," *IEEE Trans. Signal Processing*, vol. 49, no. 10, pp. 2201–2213, Oct. 2001.

[8] H. R. Künsch, "Robust priors for smoothing and image restoration," *Ann. Inst. Stat. Math.*, vol. 46, no. 1, pp. 1–19, 1994.

[9] P. Charbonnier, L. Blanc-Féraud, G. Aubert, and M. Barlaud, "Deterministic edge-preserving regularization in computed imaging," *IEEE Trans. Image Processing*, vol. 6, no. 2, pp. 298–311, Feb. 1997.

[10] P. Ciuciu, *Méthodes markoviennes en estimation spectrale non paramétrique. Applications en imagerie radar Doppler*, Phd thesis, Univ. Paris-Sud, Orsay, France, Oct. 2000.

[11] M. Cetin and W. C. Karl, "Feature-enhanced synthetic aperture radar image formation based on nonquadratic regularization," *IEEE Trans. Image Processing*, vol. 10, no. 4, pp. 623–631, Apr. 2001.